

# Molecular mechanism of CCDC106 regulating the p53-Mdm2/MdmX signal axis

Ting Zhou (✉ [tingzhou@hbut.edu.cn](mailto:tingzhou@hbut.edu.cn))

Hubei University of Technology

Xiyao Cheng (✉ [xiyaocheng@gxu.edu.cn](mailto:xiyaocheng@gxu.edu.cn))

Guangxi University <https://orcid.org/0000-0003-2161-1743>

Zhiqiang Ke (✉ [zhiqiangke@hbust.edu.cn](mailto:zhiqiangke@hbust.edu.cn))

Hubei University of Technology

Qianqian Ma (✉ [2427784681@qq.com](mailto:2427784681@qq.com))

Hubei University of Technology

Jiani Xiang (✉ [1309531207@qq.com](mailto:1309531207@qq.com))

Hubei University of Technology

Meng Gao (✉ [gaomeng@hbut.edu.cn](mailto:gaomeng@hbut.edu.cn))

Hubei University of Technology

Yongqi Huang (✉ [yqhuang@hbut.edu.cn](mailto:yqhuang@hbut.edu.cn))

Hubei University of Technology

Zhengding Su (✉ [zhengdingsu@hbut.edu.cn](mailto:zhengdingsu@hbut.edu.cn))

Hubei University of Technology <https://orcid.org/0000-0003-3558-001X>

---

## Research Article

**Keywords:** CCDC105; p53; Mdm2; MdmX; Cell proliferation

**DOI:** <https://doi.org/10.21203/rs.3.rs-2619337/v1>

**License:**  This work is licensed under a Creative Commons Attribution 4.0 International License.

[Read Full License](#)

---

1 **Molecular mechanism of CCDC106 regulating the p53-Mdm2/MdmX signal axis**

2  
3 *Ting Zhou<sup>1</sup>, Xiyao Cheng<sup>1,4,\*</sup>, Zhiqiang Ke<sup>1,5</sup>, Qianqian Ma<sup>1</sup>, Jiani Xiang<sup>1</sup>, Meng*  
4 *Gao<sup>1,2,3</sup>, Yongqi Huang<sup>1,2,3</sup> and Zhengding Su<sup>1,2,3,\*</sup>*

5  
6 *<sup>1</sup>Protein Engineering and Biopharmaceutical Sciences Group, Cooperative Innovation*  
7 *Center of Industrial Fermentation (Ministry of Education & Hubei Province), Hubei*  
8 *University of Technology, Wuhan 430068, China.*

9 *<sup>2</sup>Key Laboratory of Industrial Fermentation (Ministry of Education), Hubei University*  
10 *of Technology, Wuhan 430068, China.*

11 *<sup>3</sup>Hubei Key laboratory of Industrial Microbiology, Hubei University of Technology,*  
12 *Wuhan 430068, China.*

13 *<sup>4</sup>School of Light Industry and Food Engineering, Guangxi University, No. 100,*  
14 *Daxuedong Road, Xixiangtang District, Nanning, Guangxi, 530004, China.*

15 *<sup>5</sup>Hubei Key Laboratory of Diabetes and Angiopathy, Xianning Medical College, Hubei*  
16 *University of Science and Technology, 437100 Xianning, Hubei, China*

17  
18  
19 **To whom correspondence should be addressed:** Zhengding Su, Email:  
20 [zhengdingsu@hbut.edu.cn](mailto:zhengdingsu@hbut.edu.cn), Tel.: 86-156-23901978, ORCID: 0000-0003-3558-001X or  
21 Xiyao Cheng, Email: [xiyaocheng@gxu.edu.cn](mailto:xiyaocheng@gxu.edu.cn), Tel: 86-190-17095527, ORCID: 0000-  
22 0003-2161-1743

23  
24 **Keywords:** CCDC106; p53; Mdm2; MdmX; p21; cell cycle; apoptosis; cancer,  
25 NSCLC.

26 **Abstract**

27       The tumor suppressor p53 (p53) is regulated by murine double minute 2 (Mdm2)  
28 and its homologous MdmX in maintaining the p53 basal level. The overexpressed  
29 Mdm2/MdmX inhibit the cellular p53 activity, highly relevant to cancer occurrence.  
30 The coiled-coil domain-containing protein 106 (CCDC106) has been identified as a  
31 p53-interacting partner. However, its molecular mechanism is still elusive. Here we  
32 show that CCDC106 functions as a signaling regulator of the p53-Mdm2/MdmX axis  
33 mediated by cellular p53. We identified that CCDC106 directly interacts with the p53  
34 transactivation domain by competing with Mdm2 and MdmX. The CCDC106  
35 overexpression downregulates the cellular level of p53 and Mdm2/MdmX, and the  
36 decreased p53 reversibly downregulates the cellular level of CCDC106. Our work not  
37 only provides a molecular mechanism of CCDC106 regulating the cellular levels of p53  
38 and Mdm2/MdmX, but also suggests that the CCDC106-p53 interaction as a novel  
39 target for cancer therapy.

40

41

42

43

44

45

46

47

48

49

## 50 **Introduction**

51 The endogenous CCDC106 and p53 can be colocalized in nuclei and interact each  
52 other in vivo, promoting the degradation of p53 protein and inhibit its transactivation  
53 activity<sup>1</sup>, suggesting that CCDC106 is a negative regulator of p53 to promote cell  
54 proliferation in cancers. In ovarian cancers, the overexpression of CCDC106 promotes  
55 cell proliferation and invasion by suppressing p21 transcription through a p53-  
56 independent pathway, while the CCDC106 knockdown inhibits the expression of  
57 proliferation, invasion and EMT signaling markers in mutant p53 cells but not in wild-  
58 type p53 cells<sup>2</sup>. During cancer progression, the phosphorylation of CCDC106 by  
59 protein kinase CK2 is essential for p53 degradation and CK2 inhibitor can block the  
60 translocation of CCDC106 into the nuclei of mutant p53 cells<sup>3</sup>. In non-small cell lung  
61 cancers (NSCLC), the overexpression of CCDC106 significantly correlates with  
62 advanced TNM stage<sup>4</sup>. In two typical NSCLC cell lines that H1299 overexpresses  
63 CCDC106 but A549 expresses less CCDC106, the expression of CCDC106 upregulates  
64 the expression of Cyclin A2 and Cyclin B1, promoting cell proliferation via Akt-  
65 dependent signaling pathway<sup>4</sup>.

66 The dysfunction of p53 is a key cause of cancer development<sup>5</sup>, while CCDC106  
67 can reduce p53 stability<sup>3</sup>, suggesting that CCDC106 may be a novel target for cancer  
68 treatment. On the other hand, the phosphorylation of Mdm2 allows its entry into the  
69 nucleus where it targets p53 for degradation<sup>6,7</sup>. Thus, it is likely that the interaction of  
70 CCDC106 with p53-Mdm2/MdmX signaling pathway play an important role in cancer  
71 cell survive and drug resistance. However, it is elusive how the CCDC106 signaling  
72 regulates p53 signaling pathway. Here we identified that CCDC106 competes with  
73 Mdm2 and MdmX and directly interacts with the transactivation domain of p53. Such  
74 interaction downregulates p53 and Mdm2, promoting cell proliferation. Thus, our work

75 not only reveals a structural mechanism of CCDC106 interacting with p53, but also  
76 suggests that the CCDC106-p53 interaction is a novel target for cancer therapy.

77

## 78 **Results**

### 79 **Characterization of CCDC106 protein structure bioinformatically**

80 CCDC106 is a single polypeptide with 280 amino acid residues (**Fig. 1a**). We  
81 predicted its putative functional domains using the Simple Modular Architecture  
82 Research Tool (SMART)<sup>8</sup>. As shown in **Fig. 1b**, it contains a coiled coil domain  
83 predicted with confidence (**Table S1**). However, it is also likely that CCDC106 may  
84 have potential to constitute many other functional domains (**Table S2**), although their  
85 e-values are over threshold. As predicted with alphaFold2 program, the CCDC106  
86 structure contains a long  $\alpha$ -helix flanked by two coils at the two ends of the  $\alpha$ -helix in  
87 the N-terminal region of the CCDC106 protein, while its C-terminal region forms a  
88 compact helix-rich structure. Therefore, we arbitrarily defined these two regions as the  
89 N-terminal domain (NTD) and the C-terminal domain (CTD) of CCDC106,  
90 respectively (**Fig. 1c**).

91 To understand how CCDC106 interacts with p53 protein, we recombinantly  
92 expressed the full-length CCDC106 with FLAG and GFP tags in mammalian cells,  
93 while its NTD and CTD proteins were expressed in GST fusion form using *E. coli* cells  
94 (**Supplementary Fig. 1**). These two GST fusion proteins were used as baits to pulldown  
95 p53 in investigating the interaction between CCDC106 and p53.

96

### 97 **Expression of cellular CCDC106 is correlated with the cellular p53 level.**

98 As shown in **Fig. 2a**, CCDC106 was overexpressed in H1299, 293T and HCT116  
99 cells, while CCDC106 was marginally expressed in HepG2 cells. However, no

100 significant CCDC106 protein was detected in MCF-7 and A549 cells. We noted that  
101 both p53 and CCDC106 were overexpressed in 293T and HCT116 cells, while p53  
102 expressed at low level in MCF-7, A549 and HepG2 cells. Thus, in these cell lines, the  
103 expression of cellular p53 protein was indispensably correlated with the cellular level  
104 of CCDC106 except the H1299 cells that was supposed to have a null p53 gene. These  
105 results also suggested that the high cellular level of CCDC106 was inversely associated  
106 with the high level of cellular p53 protein. To further confirm this possibility, we  
107 knocked down the CCDC106 expression in 293T cells using siRNA approach and  
108 found that the cellular level of p53 protein significantly decreased with decreasing  
109 CCDC106 (**Fig. 2b**).

110 To examine how CCDC106 interacts with p53 protein, we conducted in vitro GST  
111 pulldown assays using GST-NTD and GST-CTD fusion proteins. As shown in **Fig. 2c**,  
112 in the presence or absence of double strand DNAs for p53 protein, the CTD domain of  
113 CCDC106 interacted with p53 protein, while the NTD domain of CCDC106 had no  
114 interaction with p53 protein (**Fig. 2d**).

115

#### 116 **CCDC106 interacts with the p53 TAD domain.**

117 Next, we would like to employ p53-null H1299 cells to investigate how CCDC106  
118 interacts p53-Mdm2/MdmX signaling pathway *in vivo*. In this work, we have firstly  
119 ensured that the full-length p53 gene is null in our H1299 cells ( **Supplementary Fig.**  
120 **2 & 3, and Supplementary Data 1-3**) as current literatures have not given a detailed  
121 information on its default p53 gene<sup>9,10</sup>. In an engineered H1299<sup>p53+</sup> cells that can express  
122 the full-length wild-type p53 protein and a truncated form of p53 protein (p53<sup>1-212</sup>), we  
123 used the GST-CTD fusion protein as a bait to conduct GST-pulldown assay. As  
124 indicated in **Fig. 2e**, both full-length p53 and p53<sup>1-212</sup> were pulled down from the

125 H1299<sup>p53+</sup> cells, indicating that the CCDC106 binding site on p53 is located within the  
126 N-terminal region of p53. We further distinguished whether CCDC106 interacts with  
127 the p53-TAD/PRD domain (i.e., p53<sup>1-93</sup>) or the p53-DBD (i.e., p53<sup>94-312</sup>). As shown in  
128 **Fig. 2f**, GST pulldown assay indicated that the CTD domain of CCDC106 interacted  
129 with the p53-TAD/PRD region but not the p53 DBD domain. To further narrow down  
130 the binding site of CCD106 on p53 protein, we did GST-pulldown assay with the p53-  
131 TAD domain (p53<sup>15-29</sup>) fused with the N-terminal domain of MdmX (N-MdmX). As  
132 shown in **Fig. 2g**, the GST-CTD fusion protein could in vitro pull down the His6-p53<sup>15-</sup>  
133 <sup>29</sup>-MdmX fusion protein that was detected by anti-His6 and anti-p53 antibodies. A  
134 similar interaction between GST-CTD and His6-p53<sup>15-29</sup>-Mdm2 was also observed (**Fig.**  
135 **2h**). To exclude the interaction between CCDC106-CTD and N-MdmX or N-Mdm2, we  
136 used the GST-N-MdmX fusion protein to pulldown a His6-tagged CTD protein (i.e.,  
137 His6-CTD), as shown in **Supplementary Fig. 4**, the CTD domain of CCDC106 had no  
138 interaction with N-MdmX. Finally, we quantitatively determined the binding affinity of  
139 p53<sup>15-29</sup> for the CTD domain with a  $K_d$  value of 0.32  $\mu$ M (**Supplementary Fig. 5**).

140

#### 141 **CCDC106 downregulates p53 and Mdm2.**

142 In the H1299<sup>p53+</sup> cells that the wild type p53 gene is fused with GFP gene, the G418  
143 induces the overexpression of the cellular p53-GFP fusion protein that is detectable  
144 with anti-p53 and anti-GFP antibodies (**Fig. 3**). As shown in **Fig. 3**, the cellular level of  
145 the p53-GFP fusion protein is downregulated with the expression of exogenous  
146 CCDC106 protein that is detected by anti-GFP and anti-FLAG antibodies. It is notable  
147 that in the H1299<sup>p53+</sup> cells the cellular level of the exogenous CCDC106 protein has no  
148 significant difference from that in the p53-null H1299 cells, indicating that the  
149 CCDC106 overexpression promotes the p53 degradation whereas p53 has no effect on

150 the cellular level of the exogenous CCDC106 protein.

151 However, we found that the endogenous CCDC106 level significantly decreased  
152 with the overexpression of exogenous CCDC106, in comparison with these of the p53-  
153 null H1299 cells and the H1299<sup>p53+</sup> cells that contained no CCDC106-expression  
154 plasmids (**Fig. 3**), although its detailed reason was unknown. Nevertheless, the cellular  
155 level of p21 protein remained in an upregulated level independent of the cellular level  
156 of CCDC106 protein. In this study, we found that the H1299 cells are typical Mdm2-  
157 overexpressing cancer cell lines (**Fig. 3**). We also noticed that the current concentration  
158 of G418 downregulated the cellular level of Mdm2, although the mechanism was  
159 unclear. Nevertheless, this biological effect was independent of the CCDC106  
160 expression (**Fig. 3**). However, when both p53 and the exogenous CCDC106 were  
161 overexpressed, the endogenous Mdm2 protein was significantly downregulated, and the  
162 endogenous CCDC106 was also downregulated (**Fig. 3**).

163

#### 164 **Overexpression of Mdm2 and MdmX downregulate p53 and CCDC106.**

165 In the H1299 cells, the expression levels of the exogenous MdmX and Mdm2 genes  
166 were distinct difference. The MdmX level was much higher than that of the Mdm2  
167 protein (**Fig. 4a**). When the exogenous MdmX and Mdm2 genes were co-expressed,  
168 the exogenous MdmX protein was further downregulated. Nevertheless, the expression  
169 of the exogenous MdmX or Mdm2 genes in the H1299 cells exhibited no significant  
170 effects on the levels of the endogenous Mdm2 protein (**Fig. 4a**). It is notable that in the  
171 H1299 cells the overexpression of the exogenous MdmX exhibited no effect on the  
172 cellular level of the endogenous CCDC106, while the expression of the exogenous  
173 Mdm2 slightly downregulated the cellular level of the endogenous CCDC106. When  
174 both exogenous MdmX and Mdm2 were co-expressed, the cellular level of the



175 endogenous CCDC106 was significantly downregulated (**Fig. 4a**).

176 By comparison, in the H1299<sup>p53+</sup> cells that the overexpression of the cellular p53  
177 protein was induced by G418 resulted in the upregulation of the cellular p21 and  
178 CCDC106 levels (**Fig. 4b**). We noticed that G418 caused the downregulation of the  
179 cellular level of the endogenous Mdm2 as also observed in **Fig. 3**. The overexpression  
180 of the exogenous MdmX gene significantly downregulated the level of cellular p53,  
181 p21 and CCDC106 proteins, accompanied by the Mdm2 downregulation. The  
182 overexpression of the exogenous Mdm2 gene could maintain a high cellular level of  
183 the endogenous Mdm2 protein. However, compared with the exogenous MdmX gene,  
184 the overexpression of the exogenous Mdm2 gene further downregulated the level of  
185 cellular p53 protein, causing a low level of the cellular p21 proteins, while the cellular  
186 level of the CCDC106 protein was maintained at a low level independent of the  
187 expression of the exogenous and endogenous Mdm2 (**Fig. 4b**). On the other hand, the  
188 co-expression of the exogenous MdmX and Mdm2 significantly downregulated the  
189 cellular level of the endogenous Mdm2, while the cellular levels of the p53, p21 and  
190 CCDC106 proteins were maintained at their low levels. Therefore, it is likely that the  
191 overexpression of either MdmX or Mdm2 enables to downregulate the cellular level of  
192 CCDC106 only mediated by p53. The overexpression of the exogenous Mdm2  
193 significantly downregulates the cellular level of p53 more than the exogenous MdmX  
194 expression. The presence of the exogenous MdmX protein significantly reduced the  
195 cellular level of the endogenous Mdm2 where this regulation was also mediated by p53.  
196 Taken together, Mdm2 and MdmX play important and different roles in regulating the  
197 cellular level of the CCDC106 protein.

198

199 **CCDC106 attenuates the p53 inhibition of the H1299 cell growth.**

200 To explore how CCDC106 affects the expression of the p53 gene and thereby  
201 controls cell cycle arrest, we treated the H1299<sup>p53+</sup> cells and their negative control cells  
202 (i.e., the H1299 cells) with G418 for 48 h in the presence or absence of the CCDC106  
203 expression vector. As shown in **Fig. 5a**, our flow cytometric assay indicated that the  
204 overexpression of p53 in the H1299<sup>p53+</sup> cells significantly affected cell cycle, causing  
205 cell arrest at the G2 stage (*the bottom middle panel*), while the H1299 cell cycles  
206 arrested at the S-stage (*the top middle panel*). When both p53 and CCDC106 were  
207 overexpressed in the H1299<sup>p53+</sup> cells, the cell amounts in the G1 and G2 stages were  
208 significantly reduced (*the bottom right panel*), compared with the H1299 cells (*the top*  
209 *right panel*), indicating that the CCDC106 overexpression attenuated the p53 function  
210 in regulating cell cycle.

211 Next, we evaluated the viabilities of the H1299 and H1299<sup>p53+</sup> cells in the presence  
212 of the CCDC106 siRNA and the Mdm2/MdmX inhibitor by use of MTT experiments.  
213 As shown in **Fig. 5b**, insignificant decrease in the H1299 cell viability was observed  
214 when the cells were transfected with the MdmX and Mdm2 expression vectors.  
215 However, the viability of the H1299<sup>p53+</sup> cells dropped much faster than that of H1299  
216 cells when p53 was overexpressed (**Fig. 5c**). When the MdmX expression vector was  
217 transfected into the H1299<sup>p53+</sup> cells, the cell viability exhibited further decreasing while  
218 the H1299<sup>p53+</sup> cells transfected with the Mdm2 expression vector started to recover their  
219 cell viability (**Fig. 5c**). The co-transfection of the MdmX and Mdm2 expression vectors  
220 significantly recovered cell viability. Furthermore, we examined the effect of the  
221 CCDC106 overexpression on the viability of the H1299<sup>p53+</sup> cells in the presence of the  
222 overexpressed p53 proteins. As shown in **Fig. 5d**, the transfection of the CCDC106  
223 expression vector with or without the transfection of MdmX expression vector  
224 exhibited no significant effect on cell viability. However, the transfection of CCDC106

225 expression vector with the transfection of Mdm2 expression vector significantly  
226 recovered cell viability (**Fig. 5d**), comparable to that of the H1299 cells (**Fig. 5b**). A  
227 similar enhancement was also observed for the H1299<sup>p53+</sup> cells that were transfected  
228 with both Mdm2 and MdmX expression vectors (**Fig. 5d**).

229 Thus, we considered examining how the inhibition of the cellular Mdm2/MdmX  
230 and CCDC106 proteins affect cell viability. As shown in **Fig. 5e**, the use of the  
231 Mdm2/MdmX dual peptide inhibitor, PMI<sup>11</sup>, significantly attenuated the effects caused  
232 by the overexpression of MdmX and Mdm2, resulting in lower cell viability.  
233 Importantly, the cell viability could be further reduced when these were treated with the  
234 CCDC106 siRNA in combination with PMI (**Fig. 5f**).

235

## 236 **Discussion**

237 To date, many studies have found that CCDC106 interacts with p53, resulting in  
238 p53 degradation in cancer cells and promoting cell proliferation<sup>1,3,4,12</sup>. In this work, we  
239 provide evidence that the C-terminal domain of the CCDC106 protein (CCDC106-CTD)  
240 directly interacts with the N-terminal domain of the p53 protein. More precisely, the  
241 CCDC106-CTD domain interacts with the TAD domain of the p53 protein.  
242 Identification of such protein-protein interaction immediately raises critical questions  
243 how CCDC106 interferes Mdm2/MdmX to bind p53 and how CCDC106 regulates the  
244 p53 signaling pathway, as Mdm2/MdmX are specific to the p53 TAD domain<sup>13,14</sup>.

245 Despite their profound relationship to p53, Mdm2 and MdmX may have quite rich  
246 and complex lives outside of p53<sup>15</sup>. In this work, it has been found that the CCDC106  
247 overexpression can significantly downregulate p53 and Mdm2. we also found that the  
248 MdmX overexpression can downregulate Mdm2 and CCDC106. Importantly, these  
249 signaling processes are solely mediated through p53. Thus, a concise interactive

250 network between CCDC106 and the p53-Mdm2/MdmX signal axis is summarized in  
251 **Fig. 6**, depicting that CCDC106 promotes the p53 and Mdm2 degradation.

252 Mdm2/MdmX are overexpressed in many cancers to impair p53 activity<sup>16,17</sup>,  
253 serving as a hot drug target for cancer therapy<sup>18-21</sup>. Considering that CCDC106  
254 competes Mdm2/MdmX for binding p53 identified from this work, therefore, we reason  
255 that the CCDC106-p53 interaction should be a promising drug target for cancer-killing  
256 in synergetic combination with drugs targeting the aberrant p53-Mdm2/MdmX  
257 interactions.

258

## 259 **Methods**

260

### 261 **Cell lines and cell cultures**

262 NCI-H1299, HCT116, MCF-7, A549, 293T and HepG2 cells were purchased from  
263 ATCC, and NCI-H1299<sup>p53+</sup> cell line was constructed in our group<sup>22,23</sup>. All kinds of cells  
264 were generally cultured in a 37 °C incubator with 5% CO<sub>2</sub> according to ATCC protocols  
265 in RPMI-1640 medium (Gibco, USA) containing 10% fetal bovine serum (FBS, Gibco,  
266 USA), supplemented with 10% serum, penicillin and streptomycin. After the cell  
267 confluency reached 80%, an individual plasmid harboring a gene encoding the Mdm2,  
268 MdmX or CCDC106 tagged with RFP protein was individually or in combination  
269 transfected for overexpressing exogenous the Mdm2-GFP, MdmX-GFP and FLAG-  
270 CCDC106-GFP fusion proteins.

271

### 272 **Transfection of siRNA**

273 The siRNAs were designed with the following two pairs of sequences.

274 siRNA\_CCDC106-1: 5'-GCGUCAAGACCCAGCUGCACA-3' and 5'-

275 UGCAGCUGGGUCUUGACGCUG-3'; siRNA\_CCDC106-2: 5'-  
276 GGACAAUGAAGGACGAUGAGA-3' and 5'-UCAUCGUCCUUCAUUGUCCGC -  
277 3'; siRNA\_negative control: 5'-UUCUCCGAACGUGUCACGUTT-3' and 5'-  
278 ACGUGACACGUUCGGAGAATT-3'. 293T, H1299 and H1299<sup>p53+</sup> cells were  
279 cultured in serum-free OPTI-DMEM medium and transfected with siRNAs using  
280 lipofectamine-RNAi MAX. The cells were collected after cultured for 72 hrs later  
281 analysis.

282

### 283 **GST pulldown experiments**

284 Pulldown experiments were carried out with GST-NTD or GST-CTD beads to  
285 pulldown p53 in cancer cell lines. GST-agarose beads were also used to examine the  
286 interaction of CTD with different domains of p53 protein, i.e., p53<sup>15-29</sup> (the p53 binding  
287 peptide, p53p), p53<sup>1-93</sup> (transactivation domain, TAD), p53<sup>94-312</sup> (DNA binding domain,  
288 DBD) and full-length p53. The GST pulldown samples were subjected to western  
289 blotting assay.

290

### 291 **Western blotting assay**

292 Total cellular proteins were extracted with RPMI lysis buffer containing 50 mM  
293 Tris (pH 7.4), 150 mM NaCl, 1% Triton-X100, 0.1% sodium deoxycholate, 0.1% SDS  
294 and 0.1% PMSF. The concentration of the protein extracts was firstly measured with  
295 Nanodrop-2000c at OD<sub>280nm</sub>, and the cellular  $\beta$ -actin contents then calibrated with  
296 mouse anti- $\beta$ -actin monoclonal antibody from ProteinTech (Wuhan, China; Cat#: HRP-  
297 60008; Gene ID 60, 100  $\mu$ g/ml) with a dilution ratio of 1:10000. Calibrated samples  
298 were separated by SDS-PAGE, while a normal molecular marker was used. Each SDS-  
299 PAGE gel was electrically transferred to a polyvinylidene difluoride (PVDF) membrane

300 (Millipore, USA). To minimize the usage of antibodies, each PVDF membrane was cut  
301 into different sections, based on the molecular weights of cellular p53, Mdm2, MdmX,  
302 p21, CCDC106 and  $\beta$ -actin and the features of their corresponding antibodies provided  
303 by their manufacturers. Each section of PVDF membranes was blocked with a 5%  
304 skimmed milk powder dissolved in TBST buffer for 1 hr at room temperature, followed  
305 by incubation individually with their corresponding primary antibodies for 2 hrs in a  
306 sealed plastic bag. After washed 3 times with TBST, the membranes were incubated  
307 with HRP-conjugated secondary antibody for 1 hr in a sealed plastic bag. Multiple  
308 sections of PVDF membranes collected and the protein bands were visualized using  
309 enhanced chemiluminescence (ECL) reagents from BioSharp (Beijing, China) on a  
310 Tanon 5200 Chemiluminescent Imager (Shanghai, China). Each blotting was repeated  
311 until a good quality image was achieved. Cellular p53 protein was blotted with a rabbit  
312 anti-TP53 polyclonal antibody IgG from CUSABIO (TX, USA; Cat#: CSB-  
313 PA15509AORB, Lot#: F0912A) with a dilution ratio of 1:4000; Cellular Mdm2 and  
314 MdmX proteins tagged with RFP were assayed with a mouse anti-RFP monoclonal  
315 antibody from Solarbio (Beijing, China; Cat#: K20016M) with a dilution ratio of  
316 1:10000. Cellular p21 protein was detected with a rabbit anti-p21 polyclonal antibody  
317 from Elabscience (Wuhan, China; Cat#: E-AB-40097) with a dilution ratio of 1:500.  
318 Cellular CCDC106 protein was detected with a rabbit anti-human CCDC106 polyclonal  
319 antibody from Abnova (Wuhan, China; Cat#: PAB19286; protein ID NP\_037433) with  
320 a dilution ratio of 1:1000; Primary antibodies were detected with either HRP-  
321 conjugated goat anti-rabbit IgG(H+L) which was from ProteinTech (Wuhan, China;  
322 Cat#: SA00001-2) with a dilution ratio of 1:10000 or HRP-conjugated goat anti-mouse  
323 IgG(H+L) which was from Biosharp (Guangzhou, China; Cat#: BL001A, 0.8 mg/ml)  
324 with a dilution ratio of 1:10000, respectively.

325

### 326 **Flow cytometric assay**

327 Cells were counted and plated in 6-well plate at  $1 \times 10^5$  cells/ml in RPMI 1640  
328 culture medium supplemented with 10% FBS. After being incubated for 3 days, Cells  
329 were washed twice with cold PBS buffer and resuspended in 1x PBS buffer at  
330  $1 \times 10^6$  cells/mL. The cell samples were incubated with Alexa Fluor488 Annexin V and  
331 PI work solution (Dead Cell Apoptosis Kit) at room temperature for 15 min. The cell  
332 cycles were analyzed by the propidium iodide (PI) reagent with a BD FACSMelody  
333 flow cytometer.

334

### 335 **Assessment of cell viability**

336 MTT assay was performed on a Synergy H1 multiplate reader (Biotek, USA) using  
337 H1299 cells and the H1299<sup>p53+</sup> cells. Cells were grown at 37°C with 5% CO<sub>2</sub> in RPMI  
338 1640 culture medium supplemented with 10% FBS until the cell density reached 90%  
339 confluency. Cells were counted and plated in 96-well plate at  $5 \times 10^3$  cells per well.  
340 After being incubated for 3 days, the medium was refreshed with RPMI 1640  
341 supplemented with 3% FBS. G418 was added in the final concentration of 50 µg/ml,  
342 and the cells continued to culture for 48 h before PMI was added in the final  
343 concentration of 1 µM in the absence or presence of siRNAs.

344 Then the MTT (5 mg/ml) solution was added in 10 µl/well. The cells were  
345 incubated for another 4 h at 37°C. After discarding culture media, the cells were washed  
346 with PBS, followed by adding 100 µl DMSO to each well. The plates were shaken on  
347 a plate shaker for 10 min. The plates were then read with the plate reader at OD<sub>490 nm</sub>.  
348 Data were processed with MicroCal Origin software (v2017, MicroCal, USA).

349

350 **Data availability**

351 The nucleotide sequence of p53 genome in H1299 cell line generated in this study  
352 have been deposited GenBank under Submission #2667019 (will be updated upon  
353 available).

354

355 **References**

356 1 Zhou, J. *et al.* Identification and characterization of the novel protein  
357 CCDC106 that interacts with p53 and promotes its degradation. *FEBS Lett* **584**, 1085-  
358 1090, doi:10.1016/j.febslet.2010.02.031 (2010).

359 2 Zhao, N. *et al.* CCDC106 promotes the proliferation and invasion of ovarian  
360 cancer cells by suppressing p21 transcription through a p53-independent pathway.  
361 *Bioengineered* **13**, 10956-10972, doi:10.1080/21655979.2022.2066759 (2022).

362 3 Ning, Y. *et al.* CK2-mediated CCDC106 phosphorylation is required for p53  
363 degradation in cancer progression. *Journal of Experimental & Clinical Cancer*  
364 *Research* **38**, 131, doi:10.1186/s13046-019-1137-8 (2019).

365 4 Zhang, X. *et al.* CCDC106 promotes non-small cell lung cancer cell  
366 proliferation. *Oncotarget* **8**, 26662-26670, doi:10.18632/oncotarget.15792 (2017).

367 5 Duffy, M. J., Synnott, N. C. & Crown, J. Mutant p53 as a target for cancer  
368 treatment. *European Journal of Cancer* **83**, 258-265, doi:10.1016/j.ejca.2017.06.023  
369 (2017).

370 6 Bononi, A. *et al.* Protein Kinases and Phosphatases in the Control of Cell Fate.  
371 *Enzyme Research* **2011**, 329098, doi:10.4061/2011/329098 (2011).

372 7 Sun, E. J., Wankell, M., Palamuthusingam, P., McFarlane, C. & Hebbard, L.



373 Targeting the PI3K/Akt/mTOR Pathway in Hepatocellular Carcinoma. *Biomedicines*  
374 **9**, doi:10.3390/biomedicines9111639 (2021).

375 8 Letunic, I., Khedkar, S. & Bork, P. SMART: recent updates, new developments  
376 and status in 2020. *Nucleic Acids Research* **49**, D458-D460,  
377 doi:10.1093/nar/gkaa937 %J Nucleic Acids Research (2020).

378 9 Iwakawa, R., Kohno, T., Enari, M., Kiyono, T. & Yokota, J. Prevalence of  
379 human papillomavirus 16/18/33 infection and p53 mutation in lung adenocarcinoma.  
380 *Cancer Science* **101**, 1891-1896, doi:10.1111/j.1349-7006.2010.01622.x (2010).

381 10 Forbes, S. A. *et al.* COSMIC (the Catalogue of Somatic Mutations in  
382 Cancer): a resource to investigate acquired mutations in human cancer. *Nucleic Acids*  
383 *Research* **38**, D652-D657, doi:10.1093/nar/gkp995 %J Nucleic Acids Research (2009).

384 11 Pazgier, M. *et al.* Structural basis for high-affinity peptide inhibition of  
385 p53 interactions with MDM2 and MDMX. **106**, 4665-4670,  
386 doi:doi:10.1073/pnas.0900947106 (2009).

387 12 Zhi, W. *et al.* HPV-CCDC106 integration promotes cervical cancer  
388 progression by facilitating the high expression of CCDC106 after HPV E6 splicing. *J*  
389 *Med Virol* **95**, e28009, doi:10.1002/jmv.28009 (2023).

390 13 Wang, X. & Jiang, X. Mdm2 and MdmX partner to regulate p53. *FEBS*  
391 *letters* **586**, 1390-1396, doi:10.1016/j.febslet.2012.02.049 (2012).

392 14 Wade, M., Li, Y. C. & Wahl, G. M. Mdm2, MdmX and p53 in oncogenesis  
393 and cancer therapy. *Nature reviews. Cancer* **13**, 83-96, doi:10.1038/nrc3430 (2013).

394 15 Klein, A. M., de Queiroz, R. M., Venkatesh, D. & Prives, C. The roles and

395 regulation of MDM2 and MDMX: it is not just about p53. *Genes Dev* **35**, 575-601,  
396 doi:10.1101/gad.347872.120 (2021).

397 16 Joerger, A. C. & Fersht, A. R. The p53 Pathway: Origins, Inactivation in  
398 Cancer, and Emerging Therapeutic Approaches. **85**, 375-404, doi:10.1146/annurev-  
399 biochem-060815-014710 (2016).

400 17 Wade, M., Li, Y.-C. & Wahl, G. M. MDM2, MDMX and p53 in  
401 oncogenesis and cancer therapy. *Nature Reviews Cancer* **13**, 83-96,  
402 doi:10.1038/nrc3430 (2013).

403 18 Munisamy, M. *et al.* Therapeutic opportunities in cancer therapy: targeting  
404 the p53-MDM2/MDMX interactions. *Am J Cancer Res* **11**, 5762-5781 (2021).

405 19 Cheng, X. *et al.* Leveraging the multivalent p53 peptide-MdmX  
406 interaction to guide the improvement of small molecule inhibitors. *Nature*  
407 *Communications* **13**, 1087, doi:10.1038/s41467-022-28721-x (2022).

408 20 Vassilev, L. T. *et al.* In vivo activation of the p53 pathway by small-  
409 molecule antagonists of Mdm2. *Science* **303**, 844-848, doi:10.1126/science.1092472  
410 (2004).

411 21 Wang, W. *et al.* Targeting MDM2 for novel molecular therapy: Beyond  
412 oncology. *Medicinal research reviews* **40**, 856-880, doi:10.1002/med.21637 (2020).

413 22 Zhou, J. *et al.* A Protein Biosynthesis Machinery Strategy for Identifying  
414 P53PTC-Rescuing Compounds as Synergic Anti-Tumor Drugs. **3**, 11048-11053,  
415 doi:10.1002/slct.201802635 (2018).

416 23 Cheng, X. *et al.* Premature termination codon: a tunable protein

417 translation approach. **73**, 80-89, doi:10.2144/btn-2022-0046 (2022).

418

419

## 420 **Acknowledgments**

421 This work was supported by the Hubei University of Technology initiative to ZDS.

422

## 423 **Authors and Affiliations**

424 Protein Engineering and Biopharmaceutical Sciences Group, Key Laboratory of  
425 Industrial Fermentation (Ministry of Education), Cooperative Innovation Center of  
426 Industrial Fermentation (Ministry of Education & Hubei Province) and Hubei Key  
427 laboratory of Industrial Microbiology, Hubei University of Technology, Wuhan 430068,  
428 China.

429 Ting Zhou, Xiyao Cheng, Zhiqiang Ke, Qianqian Ma, Jiani Xiang, Meng Gao,  
430 Yongqi Huang and Zhengding Su

431

432 School of Light Industry and Food Engineering, Guangxi University, No. 100,  
433 Daxuedong Road, Xixiangtang District, Nanning, Guangxi, 530004, China.

434 Xiyao Cheng

435

436 Hubei Key Laboratory of Diabetes and Angiopathy, Xianning Medical College, Hubei  
437 University of Science and Technology, 437100 Xianning, Hubei, China

438 Zhiqiang Ke

439

## 440 **Contributions**

441 T. Zhou, X.Y. Cheng and Z.Q. Ke carried out cell biological assays; T. Zhou, X. Y.

442 Cheng, Q.Q. Ma, and J.N. Xiang performed protein preparation; X.Y. Cheng and Z.Q.  
443 Ke performed fluorescence polarization assay; M. Gao carried out the structure  
444 predication; X.Y. Cheng, Y.Q. Huang and Z.D. Su designed the experiments; Z.D. Su,  
445 X.Y. Cheng and Y.Q. Huang wrote the paper. Z.D. Su conceived of the project.

446

#### 447 **Corresponding authors**

448 Correspondence to Zhengding Su or Xiyao Cheng.

449

#### 450 **Conflict of interest**

451 We declare that we have no conflicts of interest.

452

#### 453 **Supporting information available**

454 Supplementary tables and figures are available in the online version of this paper.

455

456

457

458

459

460

461

462

463

464

465

466

467

468 **Figure legends**

469

470 **Fig. 1. Prediction of the structure domains of CCDC106 protein.** **a.** Amine acid  
471 sequence of human CCDC106. **b.** Potential domains in CCDC106 predicted by SMART  
472 program. Putative domains are described in *Supplementary Information*. **c.** Putative  
473 three-dimensional structure of CCDC106 was predicted with alphaFold2 program.  
474 Source data for **c** are provided as a Source Data file.

475

476 **Fig. 2. Correlation between CCDC106 and p53.** GST: GST protein; Input: the cell  
477 extracts; GST-CTD: the GST-CTD fusion protein; Beads: GST agarose beads; p53: the  
478 full-length p53 protein, p53<sup>1-212</sup>: the N-terminal segment of p53 containing TAD, PRD  
479 and partial DBD domain; p53<sup>1-93</sup>: the TAD and PRD domains; p53<sup>94-312</sup>: the DBD  
480 domain of p53, p53<sup>15-29</sup>: the p53 TAD domain, N-MdmX and N-Mdm2: the N-terminal  
481 domains of MdmX and Mdm2, respectively. **a.** The cellular levels of endogenous  
482 CCDC106 and p53 proteins in H1299, 293T, HCT116, MCF-7, A549 and HepG2 cells  
483 were assayed by western blotting. **b.** Knockdown of the endogenous CCDC106 in 293T  
484 cells downregulates the cellular level of endogenous p53. **c.** In vitro pulldown of p53  
485 protein with the GST-CTD fusion protein was detected with anti-p53 polyclonal  
486 antibody. **d.** No obvious interaction was detected in vitro between p53 and the GST-  
487 NTD with GST-pulldown assay that was detected with anti-p53 polyclonal antibody. **e.**  
488 Pulldown of the full-length and a N-terminal segment of p53 with the GST-CTD fusion  
489 protein. **f.** Pulldown of p53<sup>1-93</sup> but not p53<sup>94-312</sup> with the GST-CTD fusion protein. Inputs  
490 were the cell extracts of *E. coli* cells expressing p53<sup>1-93</sup> or p53<sup>94-312</sup>. **g** & **h.** Pulldown of  
491 p53<sup>15-29</sup> in the N-MdmX or N-Mdm2 fusion forms with the GST-CTD fusion protein.  
492 Blots in each subgroup were made from either the same gel or different gels with similar

493 exposure time. Source data for **a – h** are provided as a Source Data file.

494

495 **Fig. 3. CCDC106 downregulates cellular p53 and Mdm2 in H1299<sup>p53+</sup> cells.** Assays  
496 were done with western blotting in the presence or absence of G418. G418: inducer of  
497 the p53 expression in the H1299<sup>p53+</sup> cells; PL(CCDC106): the expression plasmid of  
498 CCDC106; GFP(CCDC106) and FLAG(CCDC106): CCDC106 fused with FLAG and  
499 GFP tags; The p53 protein was detected with p53 polyclonal antibody and anti-GFP tag  
500 monoclonal antibody. CCDC106 was detected with CCDC106 polyclonal antibody,  
501 anti-GFP tag monoclonal antibody and anti-FLAG monoclonal antibody. p21 and  
502 Mdm2 were detected with their polyclonal antibodies. Actin was used a control. All  
503 blots were made from the same gel. Source data are provided as a Source Data file.

504

505 **Fig. 4. Mdm2 and MdmX downregulate cellular CCDC106 via p53.** PL-MdmX and  
506 PL-Mdm2: plasmids harboring MdmX or Mdm2 genes, respectively;  
507 RFP(MdmX/Mdm2): MdmX-RFP and Mdm2-RFP fusion proteins, respectively.  
508 Exogenous MdmX and Mdm2 were detected with their polyclonal antibodies.  
509 Endogenous Mdm2 was detected with its polyclonal antibody. The p53 was detected  
510 with p53 polyclonal antibody. Endogenous p21 and CCDC106 proteins were detected  
511 with p21 and CCDC106 polyclonal antibodies, respectively. Actin was used a control.  
512 Blots in **a** and **b** were made from two different gel, respectively. Source data for **a – b**  
513 are provided as a Source Data file.

514

515 **Fig. 5. Overexpression of CCDC106 attenuates the p53 function on cell**  
516 **proliferation.** All the cells were cultured in the presence of 50 µg/mL G418 for  
517 inducing the p53 overexpression. **a.** A flow cytometric assay of H1299<sup>p53+</sup> cells

518 overexpressing CCDC106 in comparison with the H1299 cells. Control: no G418 and  
519 PL-CCDC106 plasmid. **b-f.** Effects of the Mdm2/MdmX dual inhibitors (PMI) and the  
520 CCDC106 siRNA on the H1299<sup>p53+</sup> cell viability in comparison with that of the H1299  
521 and H1299<sup>p53+</sup> cells. *Dark*: negative control; *light grey*: transiently transfected with the  
522 MdmX expression vector; *Dark grey*: transiently transfected with the Mdm2 expression  
523 vector; *Blank*: transiently transfected with both MdmX and Mdm2 expression vectors.  
524 n = 3 independent experiments, p>0.05 compared with the control group. **b.** H1299  
525 cells. **c.** H1299<sup>p53+</sup> cells. **d.** The H1299<sup>p53+</sup> cells were transfected with the CCDC106  
526 expression plasmid. **e** The H1299<sup>p53+</sup> cells were treated with 1 μM of PMI. **f.** The  
527 H1299<sup>p53+</sup> cells were treated with the CCDC106 siRNA and 1 μM of PMI. Source data  
528 for **b – f** are provided as a Source Data file.

529

530 **Fig. 6. A signaling map depicting the CCDC106-p53-Mdm2 interactions regulating**  
531 **cell proliferation.** This signaling map was constructed by combining the data from this  
532 work with previously published data <sup>6,7</sup>. IR: irradiation; DSB: DNA double strand break;  
533 ROS: reactive oxygen species; AKT: Akt serine/threonine kinase; ATM: ataxia  
534 telangiectasia mutated kinase; NBS1: Nijmegen breakage syndrome 1; Ac: acetyl group;  
535 T: threonine; S: serine; K: lysine; U: ubiquitin. p27: Cyclin dependent kinase  
536 inhibitor p27.

537

Fig. 1, Zhou et al.,

a

```
      10      20      30      40      50
KNDRSSRRRT MKDDETFEIS IPFDEAPHLD PQIFYSLSPS RRNFEEPPEA

      60      70      80      90     100
ASSALALMNS VKTQLHMALE RNSWLQKRIE DLEEERDFLR CQLDKFISSA

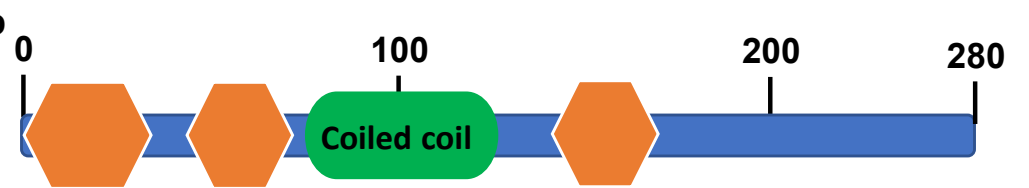
     110     120     130     140     150
RMEAEDHCRM KPGPRRMEGD SRGGAGGEAS DPESAASSLS GASEEGSASE

     160     170     180     190     200
RRRQKQKGGG SRRRFGKPKA RERQRVKADG GVLCRYKKIL GTFQKLKSMS

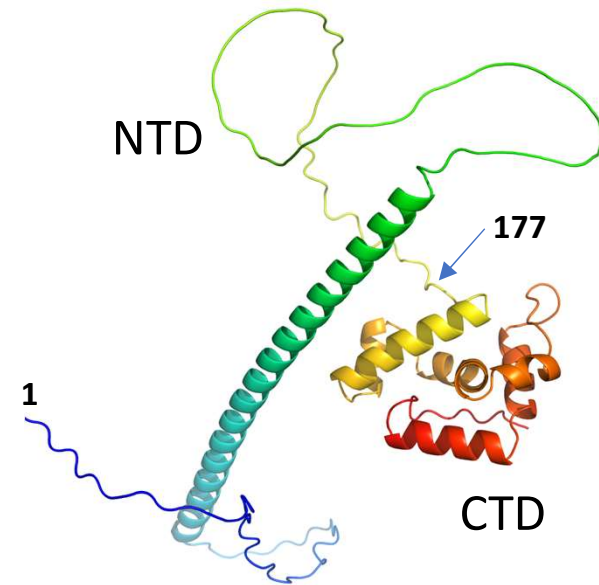
     210     220     230     240     250
RAFEHHRVDR NTVALTTPIA ELLIVAPEKL AEVGEFDPSK ERLLYSRRC

     260     270     280
FLALDDETLK KVQALKKSKL LLPITYRFKR
```

b



c





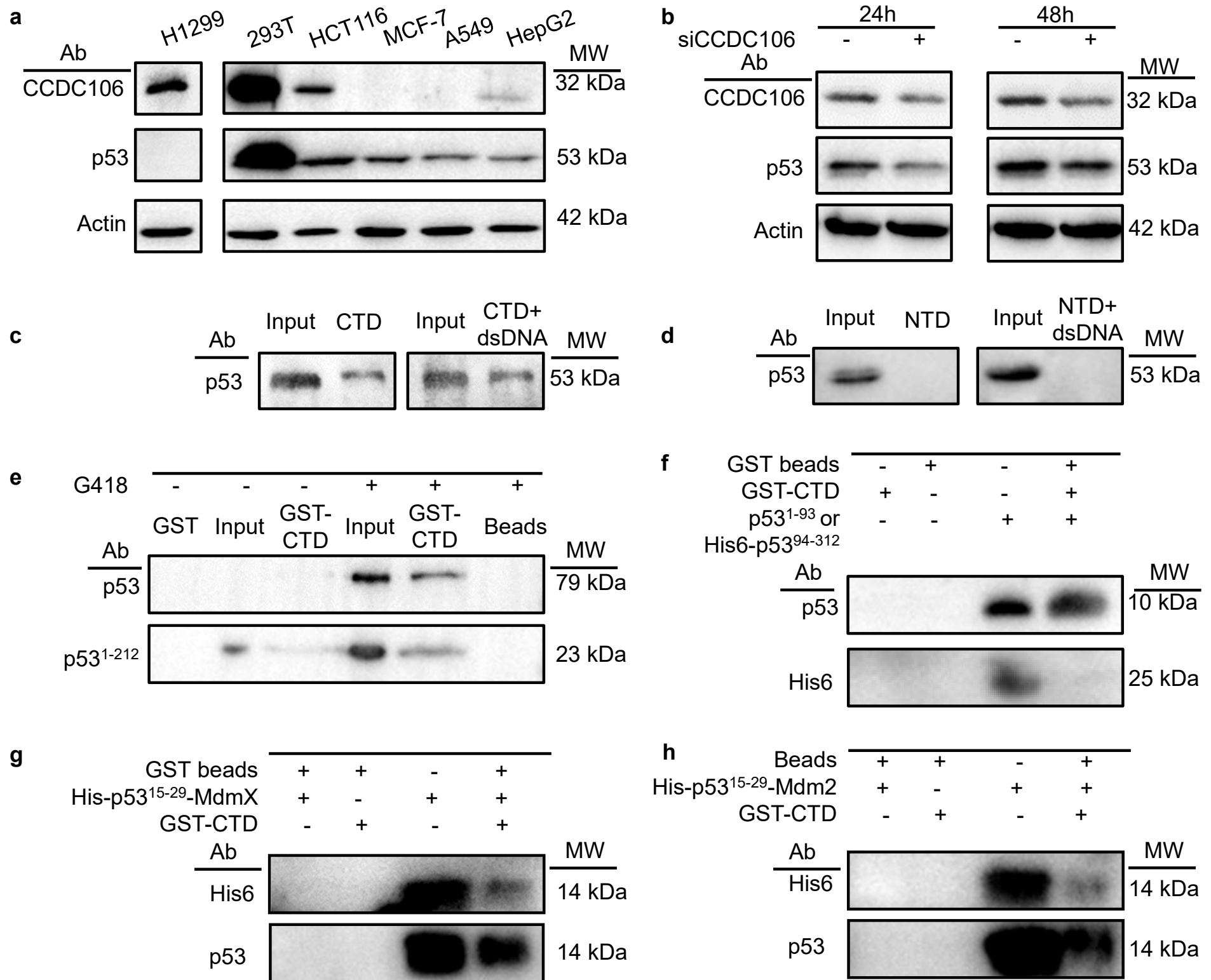


Fig. 3, Zhou et al.,

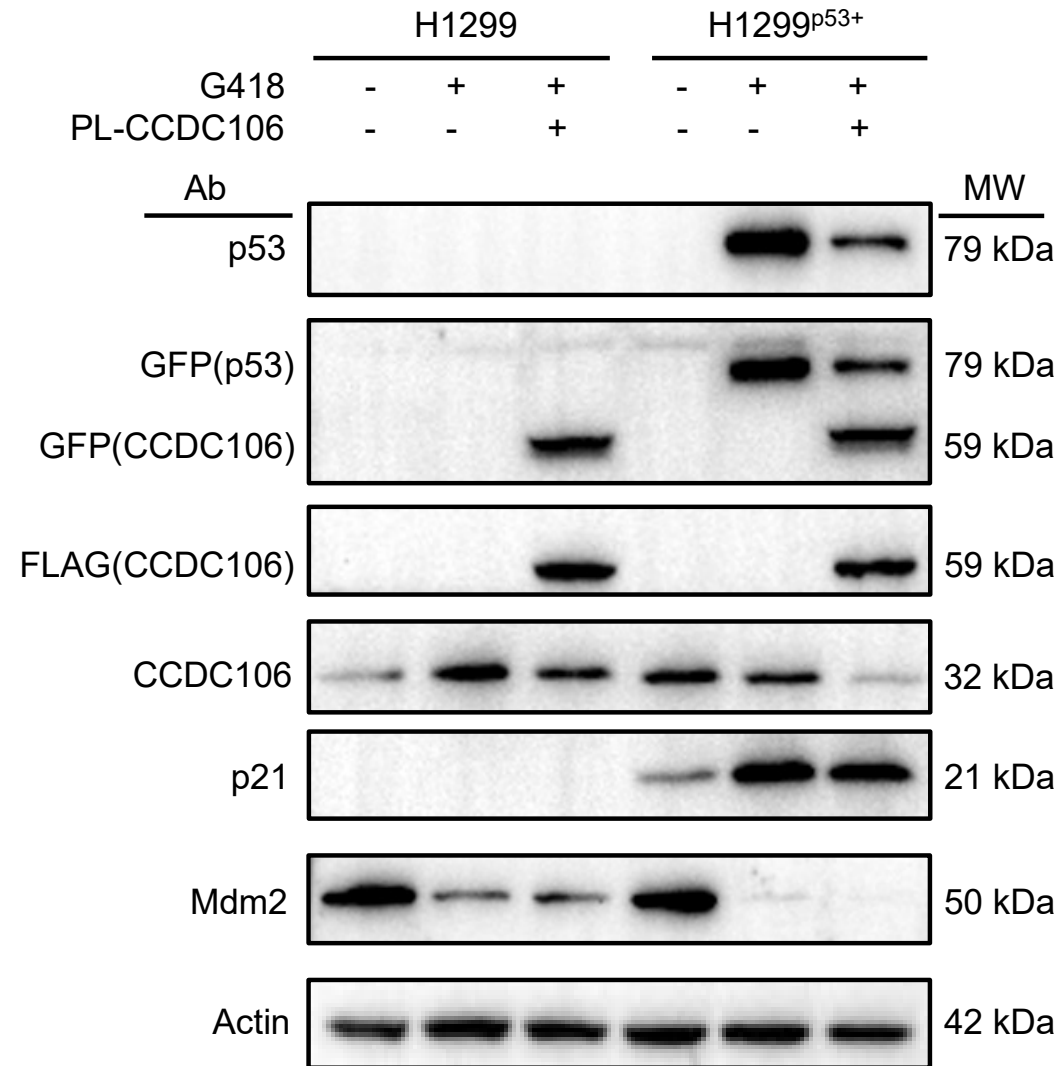


Fig. 4, Zhou et al.,

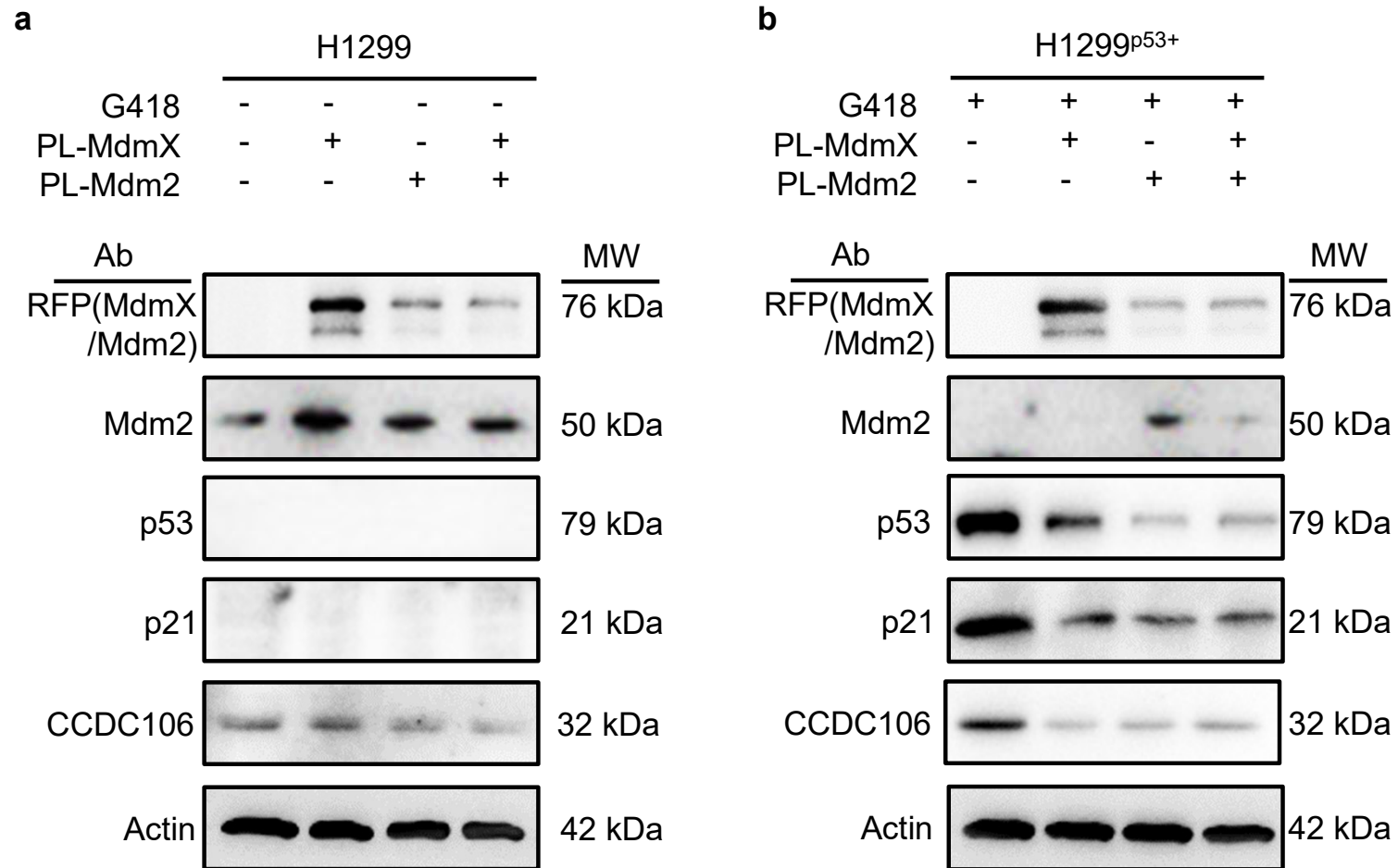


Fig. 5, Zhou et al.,

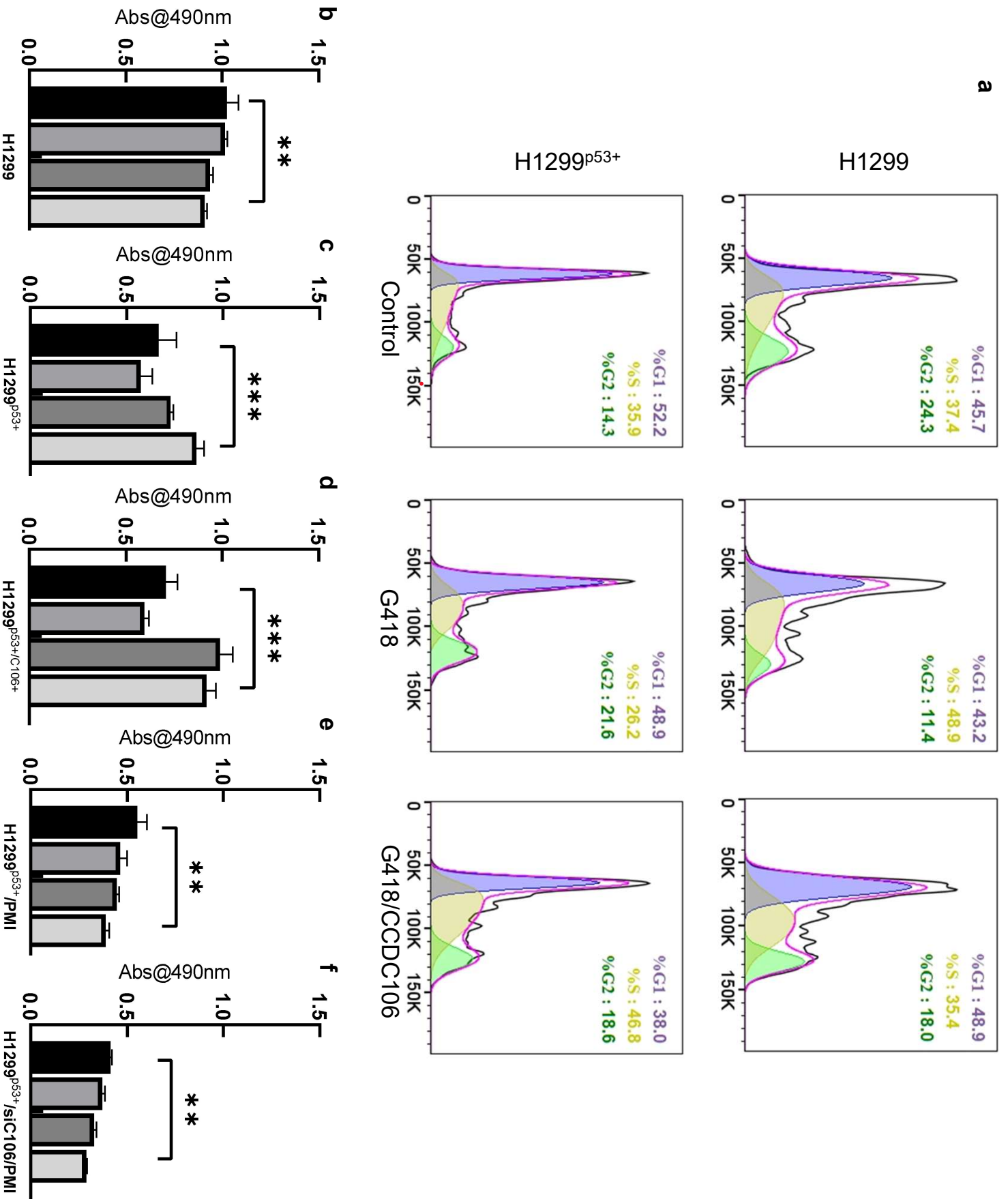
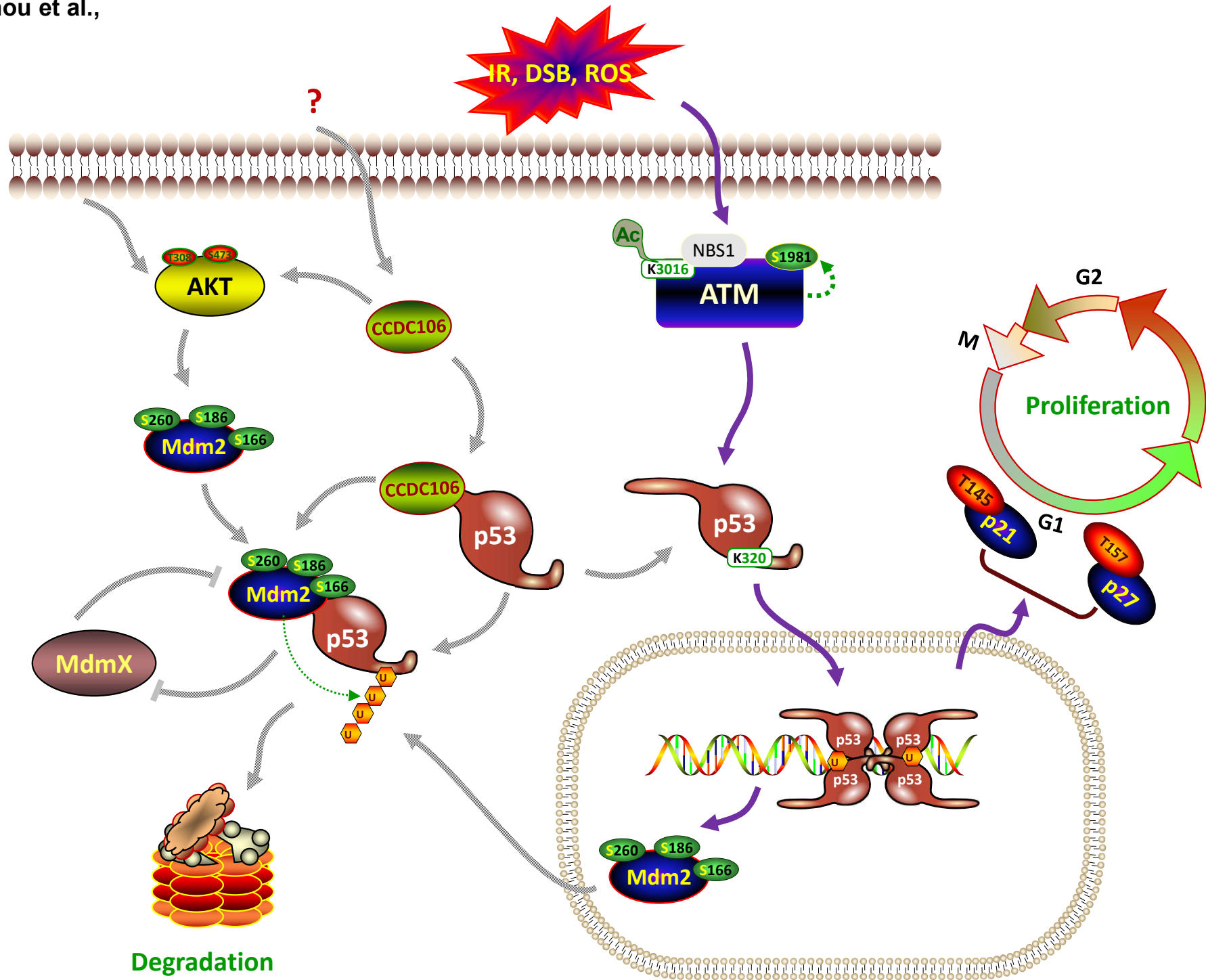


Fig. 6, Zhou et al.,



***Supplementary Information for***

**Molecular mechanism of CCDC106 regulating the p53-Mdm2/MdmX signal axis**

*Ting Zhou<sup>1</sup>, Xiyao Cheng<sup>1,2,\*</sup>, Zhiqiang Ke<sup>1,3</sup>, Qianqian Ma<sup>1</sup>, Jiani Xiang<sup>1</sup>, Meng Gao<sup>1</sup>, Yongqi Huang<sup>1</sup> and Zhengding Su<sup>1,\*</sup>*

*<sup>1</sup>Protein Engineering and Biopharmaceutical Sciences Group, Key Laboratory of Industrial Fermentation (Ministry of Education), Cooperative Innovation Center of Industrial Fermentation (Ministry of Education & Hubei Province) and Hubei Key laboratory of Industrial Microbiology, Hubei University of Technology, Wuhan 430068, China.*

*<sup>2</sup>School of Light Industry and Food Engineering, Guangxi University, No. 100, Daxuedong Road, Xixiangtang District, Nanning, Guangxi, 530004, China.*

*<sup>3</sup>Hubei Key Laboratory of Diabetes and Angiopathy, Xianning Medical College, Hubei University of Science and Technology, 437100 Xianning, Hubei, China*

**To whom correspondence should be addressed:** Zhengding Su, Email: zhengdingsu@hbut.edu.cn, Tel.: 86-156-23901978, ORCID: 0000-0003-3558-001X or Xiyao Cheng, Email: xiyaocheng@gxu.edu.cn, Tel: 86-190-17095527, ORCID: 0000-0003-2161-1743

**Keywords:** CCDC106; p53; Mdm2; MdmX; p21; cell cycle; apoptosis; cancer, NSCLC.

## Supplementary Results

### Bioinformatic characterization of CCDC106 protein

As its biological function has not been thoroughly investigated, we use the Simple Modular Architecture Research Tool (SMART) <sup>1</sup> to predict its putative domains. As shown in **Fig. 1b**, it contains a coiled coil domain predicted with confidence (**Supplementary Table 1**). However, it is also likely that CCDC106 may have potential to constitute other functional domains, such as Basic region leucine zipper (BRLZ), Parathyroid hormone (PTH), Repeats in fly CG4713, worm Y37H9A.3 and human FLJ20241 (DM14), Suppressor of glucose by autophagy (SOGA), Homeobox associated leucine zipper (HALZ), Worm-specific N-terminal domain (WSN), Helicase and RNaseD C-terminal (HRDC) domains, although their e-values are over threshold (**Supplementary Table 2**).

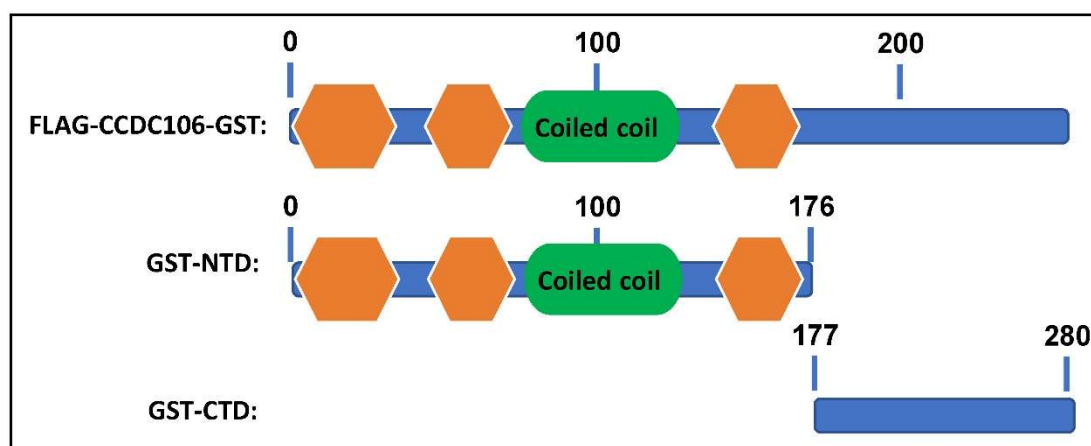
**Supplementary Table 1. Confidently predicted of domains, repeats, motifs and features of CCDC106**

<b>Structure property</b>	<b>Sequence start</b>	<b>Sequence end</b>	<b>E-value</b>
Low complexity	45	57	N/A
Coiled coil	63	101	3.9e-100
Low complexity	133	150	N/A

**Supplementary Table 2. Possible structure features of CCDC106**

<b>Name</b>	<b>Start</b>	<b>End</b>	<b>E-value</b>	<b>Reason</b>
SOGA	58	157	0.21	threshold
BRLZ	43	95	32.2	threshold
PTH	49	85	60.1	threshold
HALZ	241	278	583	threshold
WSN	187	249	683	threshold
HRDC	186	265	893	threshold
DM14	55	114	1140	threshold

As predicted using alphaFold2 program, the CCDC106 structure contains a long  $\alpha$ -helix flanked by two coils at the two ends of the  $\alpha$ -helix in the N-terminal region of the CCDC106 protein, while its C-terminal region forms a compact helix-rich structure. Therefore, we arbitrarily define these two regions as the N-terminal domain (NTD) and the C-terminal domain (CTD) of CCDC106, respectively (**Fig. S1**).



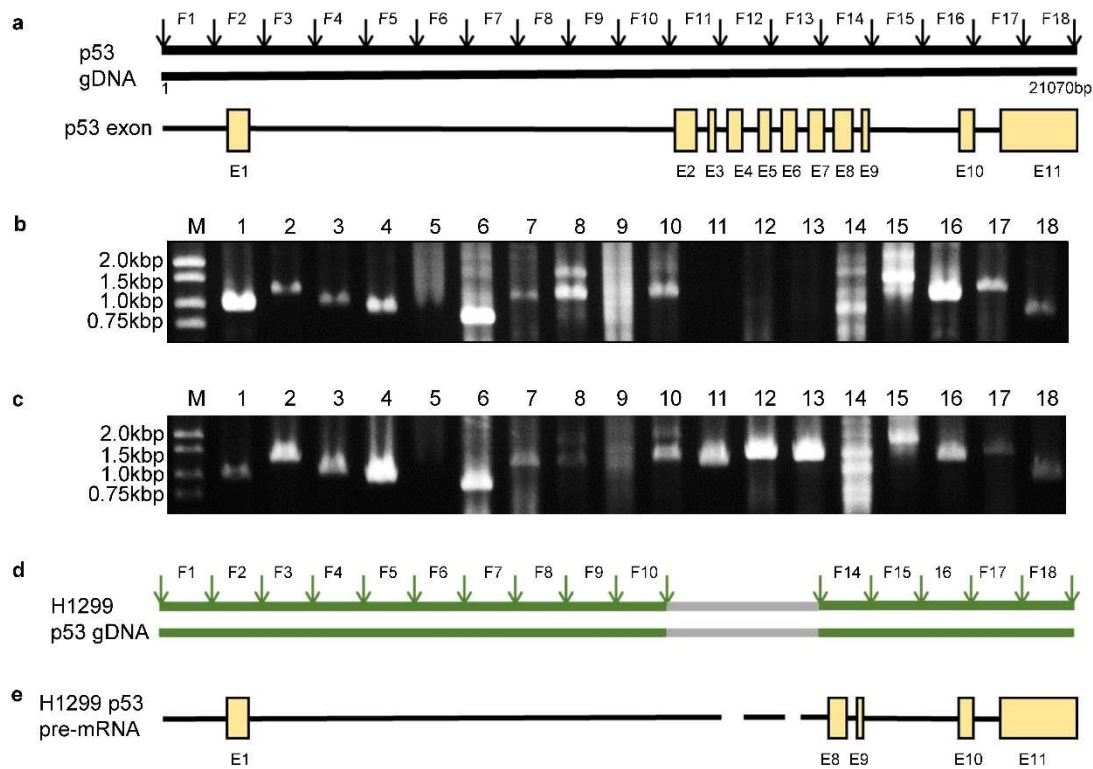
**Supplementary Fig. 1. Dissection of CCDC106 structure for expression in GST fusion protein.**

### **Examination of p53 gene in H1299 genome**

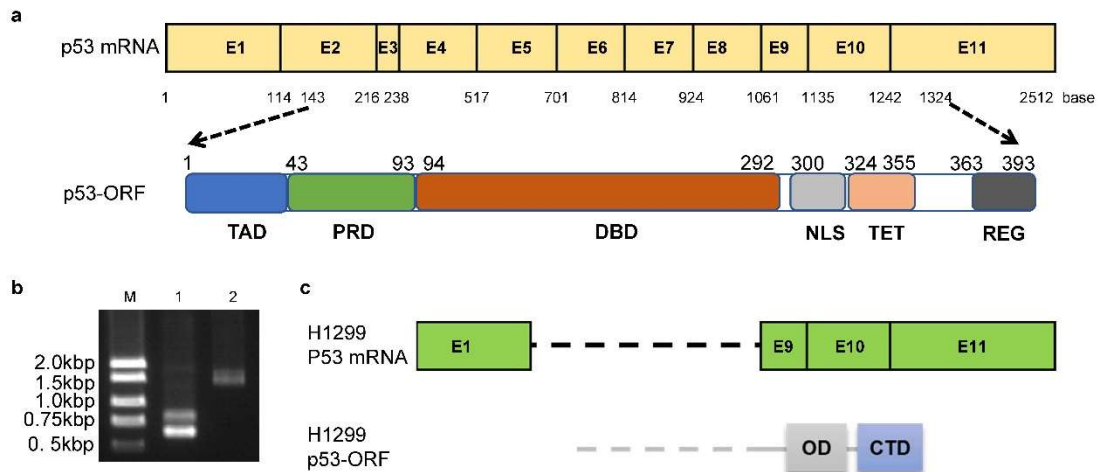
In normal human cells, the loco of the wild type p53 gene is in the 17<sup>th</sup> chromosome with a length of 21070 bp embedded in a long promotor region and the p53 genome. The p53 genome contains 11 exons and 10 introns (**Supplementary Fig. 2**). We used 18 pairs of specific primers to amplifyp53 DNA fragments from the H1299 genome using the p53 genome of the 293T cells as template. As shown in **Supplementary Fig. 2b**, the fragments 11, 12 and 13 were not detected from the H1299 genome, while these three fragments could be amplified from the HCT116 genome (**Supplementary Fig. 2c**) that contains a wild type p53 gene <sup>2</sup>. Thus, the p53 genomic DNA in H1299 cells was missing the entire DNA sequence covering the region from exon 2 to exon 7



(Supplementary Fig. 2d & 2e). After amplified DNA fragments were evaluated by DNA sequencing, we found that all the amplified fragments matched the DNA sequences expected from human genomics and the p53 genome of HCT116 cells (see Supplementary Data 1).



**Supplementary Fig. 2. DNA sequencing of the p53 gene in H1299 cell line.** **a.** A schematic structure of p53 genome from human genomics. F1-F18 represent 18 fragments for designing primers for sequencing the p53 gDNA. E1-E11 represent 11 annotated exons in native p53 gDNA. **b.** Agarose gel imaging of the PCR fragments for F1-F18 using the H1299 gDNA as template. **c.** Agarose gel imaging of the PCR fragments for F1-F18 using the HCT116 gDNA as template (positive control). **d.** A cartoon summarizes DNA sequencing results. *Green*: detected segments and *grey*: undetected segments in the p53 gDNA from the H1299 genome. **e.** A cartoon represents the primary mRNA of p53 in H1299 cells. Boxes represent existed exons.



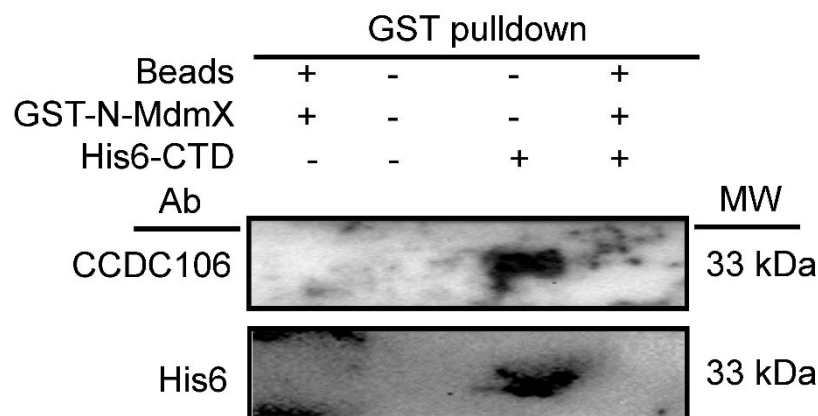
**Supplementary Fig. 3. Determination of p53 mRNA in H1299 cells.** **a.** The wild type p53 mRNA from human genomics is composed of 11 exons. An open reading frame (ORF) of matured p53 protein is deduced based on the p53 mRNA. TAD: Transactivation domain; PRD: Proline-rich domain; DBD: DNA binding domain; NLS: Nuclear localization sequence; TET: Tetramerization domain; REG: Regulation domain. **b.** The p53 cDNA reverse-transcribed from the H1299 mRNA sample was visualized by agarose gel.

The wild type p53 gene is composed of exons 2-11 (**Supplementary Fig. 3a**). And a matured p53 mRNA encodes a full-length polypeptide of 393 residues, consisting of multiple functional domains including a transactivation domain (TAD), an proline-rich domain (PRD), DNA-binding domain (DBD), nuclear localization sequence (NLS), Tetramerization domain (TET) and C-terminal regulatory domain (REG)<sup>3</sup> (**Supplementary Fig. 3a**). To examine whether an p53 fragment exist in H1299 cells, we isolated the total RNAs from the H1299 cell extracts and amplified p53 cDNA with two pairs of primers designed based on native p53 mRNA sequence. One pair of primers was used to amplify the region from promotor to stop codon and other pair was used to

amplify whole region from promotor to terminator. As shown in **Supplementary Fig. 3b**, the resultant PCR products was shorter than expected length. These PCR bands were further subcloned with a TOPO-Blunt vector for DNA sequencing. The DNA sequencing results revealed a shorter p53 mRNA that contains only exons 1, 9, 10 and 11 (**Supplementary Fig. 3c** and **Supplementary data 1-3**). This short mRNA can be only translated into a short peptide containing TET and REG domains (**Supplementary Fig. 3c**). Thus, our data revealed that H1299 cells cannot express a full-length p53 protein.

#### No interaction between CCDC106-CTD and N-MdmX

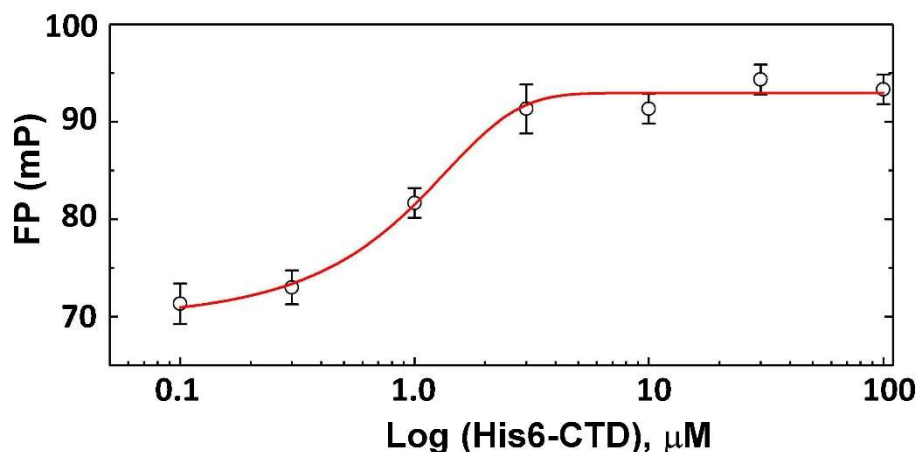
To exclude the interaction between CTD and N-MdmX or N-Mdm2, we used the GST-N-MdmX fusion protein to pulldown a His-tagged CTD protein (i.e., His6-CTD), as shown in **Supplementary Fig. 4**, the CTD domain of CCDC106 had no interaction with MdmX.



**Supplementary Fig. 4. GST pulldown assay of CCDC106-CTD.** Beads: GST agarose beads; GST-N-MdmX: the GST and N-MdmX fusion protein; His6-CTD: His6-tagged CTD protein. CCDC106 protein was detected CCDC106 polyclonal antibodies. Source data are provided as a Source Data file.

### Quantitation of the interaction of CCDC106-CTD with p53<sup>15-29</sup>

We quantitatively determined the binding affinity of p53<sup>15-29</sup> for the CTD domain with a  $K_d$  value of 0.32  $\mu\text{M}$  (Supplementary Fig. 5).



**Supplementary Fig. 5. Determination of the binding affinity of p53<sup>15-29</sup> with the CTD domain of CCDC106 using fluorescence polarization (FP) assay.** Source data are provided as a Source Data file.

### Supplementary methods

#### Materials

The cDNA of the human CCDC106 gene was synthesized by GenScript (Wuxi, China) and sub-cloned to the pcDNA3.0 plasmid where the FLAG tag and the RFP tag were inserted at its 5-terminal and at its 3'-terminal ends, respectively. Lipofectamine 2000 was purchased from Invitrogen (Shanghai, China). The peptides including PMI and fluorescein-labeled p53p (Flu-p53p) were synthesized by TOPE Biotech (Shanghai, China). NCI-H1299, HCT116, MCF-7, A549, 293T and HepG cells were purchased

from ATCC, and NCI-H1299<sup>p53+</sup> cell line was constructed in our group<sup>4,5</sup>.

The primers used in this study were synthesized by GenScript (Nanjing, China). The siRNAs were designed and synthesized by Genepharma (Suzhou, China). Genomic DNA extraction kit, plasmid mini-prep kit and PCR cleanup kit were purchased from Tiangen Biotech (Beijing, China). RNA extraction kit RNeasy® Mini Kit was purchased from QIAGEN China (Shanghai, China). RT-PCR kits and Taq Mix were purchased from Vazyme Biotech (Nanjing, China). TOPO-Blunt Simple Cloning Kit was purchased from Yisheng Biotech (Shanghai, China). MTT (3-[4,5-dimethylthiazol-2-yl]-2,5 diphenyl tetrazolium bromide) was obtained from Biofroxx (Guangzhou, China).

### **Protein expression and purification from *E. coli* cells**

The DNA sequences of the N-terminal domain (1-176) and C-terminal domain (177-280) of CCDC106 were optimized with *E. coli* bias codons and synthesized by GenScript (Wuxi, China) and sub-cloned to the pGEX-6P-1 plasmid. The wild-type p53 and its TAD domain (1-93) and DBD domain (94-312) were subcloned in a modified pET28b plasmid that its thrombin cleavage site was substituted with the Tev protease cleavage site<sup>6</sup>.

Recombinant proteins were prepared in *E. coli* BL21 (*DE3*) cells. Cells were grown in LB medium containing kanamycin (34 µg/mL) for modified pET28b vector or ampicillin (50 µg/mL) for pGEX-6P-1 vector and induced with 0.4 mM IPTG at 18°C for 12 h.

To purify His-tagged protein, cells were harvested by centrifugation at 5,000 ×g for 30 min, resuspended in a buffer containing 10 mM Tris-HCl, 40 mM NaCl, 2 mM β-mercaptoethanol, 2 mM imidazole, pH 8.0 (Buffer A), and lysed by sonication and

homogenization, followed by spinning at 18,000  $\times g$  for 30 min. The supernatant was loaded onto a 5 mL Ni-NTA agarose column (Qiagen, USA) and His-tagged protein was competitively eluted using a gradient of Buffer A mixed with Buffer B containing 10 mM Tris-HCl, 40 mM NaCl, 2 mM  $\beta$ -mercaptoethanol, 300 mM imidazole, pH 8.0. The eluate was diluted in 20 times with a buffer containing 20 mM sodium citrate (pH 6.5), 10% glycerol, 2 mM  $\beta$ -mercaptoethanol.

To purify GST-tagged protein, cells were harvested by centrifugation at 5,000  $\times g$  for 30 min, resuspended in 1x PBS buffer and lysed by sonication and homogenization, followed by spinning at 18,000  $\times g$  for 30 min. The supernatant was loaded onto a 5 mL GST agarose column (GE, USA) and GST-tagged protein was competitively eluted using 1x PBS buffer containing 10 mM glutathione. The eluate was desalted with a 1x PBS buffer. All purified protein samples were freshly frozen in liquid nitrogen, and kept at -80 °C.

### **DNA sequencing of p53 genomic gene in H1299 cells**

The genomic DNA of H1299 and HCT116 cells was extracted with the cell genome extraction kit, and the 53 genome was divided into 18 fragments according to the genome data on NCBI (Genebank ID: 7157). PCR was used to identify whether each fragment existed in H1299, and HCT116 was used as a control. PCR was carried out with *Taq* DNA polymerase in 50  $\mu$ L reaction mixture, which contained 25  $\mu$ L of 2  $\times$  Taq mix, 2 nM primers and 10 ng template DNA.

The total RNA of H1299 cells was extracted using the RNA extraction kit, and immediately reverse transcription PCR (RT-PCR) was performed to obtain the cDNA library of H1299, and then each putative fragment of p53 gene were amplified with designed primers (**Supplementary Table 3**). PCR products were evaluated by agarose

gel electrophoresis. The fragments obtained by the above PCR were purified and ligated with TOPO-Blunt vector. The ligation mixture was transformed into *E. coli* DH5 $\alpha$  competent cells for selecting correct colonies. After cultured for 12 hours, a single colony was picked and identified using colony PCR with primers M13-F: 5'-TGTA AACGACGGCCAGT-3' and M13-R: 5'-CAGGAAACAGCTATGACC-3'. PCP products were directly used for DNA sequencing.

**Supplementary Table 3. Primers for sequencing p53 genomic DNA and cDNAs**

Primer	Sequence (5'-3')
1	TGCTCAAGACTGGCGCTA
2	AAAAAGAAATGCAGGCGGAGAATAG
3	CGATGAGAGGGGAGGAGAGAGA
4	ATATATAACAACATGAACGAAT
5	GGAATCATAACATTATGTG
6	CAAAGAAAAAAGAAAATAGC
7	CCTTTCTCTACTGAATGCTTT
8	CTGGCCTATTTATCCTTTTT
9	ATGCAACAGCTAACCAATTTT
10	TAGGCCTCCCAAAGTGCTGGCAT
11	GTCGGAGTTCCACTAGCAGCA
12	GCGTGAGACATCGGGCCACTAA
13	GCCTGGGCGACAGAGCAAGACTGT
14	ATTACAGGCGCCCACCACTACA
15	TGAGACCAACCTAACATGGTG
16	TACCTAGTACTCTGTGTATTA
17	GCAGAAAGAGCTAACCTTTGTT
18	CGGAGTCTCGCCCTGTCACC
19	AATCCCAGCTACTCAGGAAGT
21	GGGCTGAGGAGTGTCGAAGA
22	TGGGTCTTCAGTGAACCATTG
23	CTTTTCACCCATCTACAGTCC
24	GCAACCAGCCCTGTCGTCTCT
25	GCACATGACGGAGGTTGTGAG
26	CTACCTGTCCCATTTAAAAA
27	TCCTCCACCTACCTGGAGCTG
28	GCTATGATCACATCACTGTAA
29	GCCTGCCTAGCCTACTTTTAT
30	TGAGCCAGTGCGCCTGGCCTTTT
31	AGCATGGTTGCATGAAAGGAG
32	TCAACCGGAGGAAGACTAAAA
33	CCATTCTCATCCTGCCTTCAT
34	TGGTTAGTACGGTGAAGTGGG

35 GGAGATGTAAGAAATGTTCTT  
36 TGGCAGCAAAGTTTTATTGTA  
p53-promoter-F CTCAAAAGTCTAGAGCCACCG

---

### Fluorescence polarization (FP) assay

Fluorescence polarization assay was done using black, low-protein-binding 96-well plates (Corning, NY) in a total volume of 100  $\mu$ L per well of 20 mM phosphate (pH 6.8), 200 mM NaCl, and 1 mM DTT. One nM of fluorescein-p53p (fluorescein-GSGSSQETFSDLWKLLPEN, Flu-p53p) titrated with GST-CTD and FP readings were taken with a 555 nm excitation filter and a 632 nm static and polarized filter on a BioTek H1 multiplate reader with Gen5 software. All FP data were fitted with Origin 2017 for obtaining  $K_d$  values.

### Supplementary References

1 Letunic, I., Khedkar, S. & Bork, P. SMART: recent updates, new developments and status in 2020. *Nucleic Acids Research* **49**, D458-D460, doi:10.1093/nar/gkaa937 %J Nucleic Acids Research (2020).

2 Leroy, B. *et al.* Analysis of TP53 Mutation Status in Human Cancer Cell Lines: A Reassessment. *Human Mutation* **35**, 756-765, doi:<https://doi.org/10.1002/humu.22556> (2014).

3 Zhang, S. C. L. H. B. L. S. A. A. A. U. T. X. E.-D. W. S. T. I. A. S. f. T. T. o. W.-T. & Mutant p53 in, C. *Biomolecules* **12** (2022).

4 Zhou, J. *et al.* A Protein Biosynthesis Machinery Strategy for Identifying P53PTC-Rescuing Compounds as Synergic Anti-Tumor Drugs. **3**, 11048-11053, doi:<https://doi.org/10.1002/slct.201802635> (2018).



5 Cheng, X. *et al.* Premature termination codon: a tunable protein translation approach. **73**, 80-89, doi:10.2144/btn-2022-0046 (2022).

6 Qin, L. *et al.* Effect of the Flexible Regions of the Oncoprotein Mouse Double Minute X on Inhibitor Binding Affinity. *Biochemistry* **56**, 5943-5954, doi:10.1021/acs.biochem.7b00903 (2017).